Electronic structure and core exciton of hexagonal boron nitride

John Robertson*
Department of Physics, University of Illinois, Urbana, Illinois 61801
(Received 15 March 1983)

A new tight-binding band calculation is presented for the layer compound boron nitride which correctly describes the widths of both σ and π bands. The binding energy and wave function of the B $1s \rightarrow 2p$ core exciton are studied. The core exciton is found to be small and bound by the medium-range part of the core-hole potential. Its binding energy far exceeds the interlayer band dispersion at the conduction-band minimum. Its incomplete π-like polarization is found to be due to a small admixture of B σ states from adjacent layers into the A_1^- final state.

I. INTRODUCTION

Hexagonal boron nitride (h-BN) is one of the most anisotropic layer compounds. Its electronic structure has been studied by optical reflectivity and absorption,[1-3] photoemission,[4,5] x-ray emission,[6-8] energy-loss[9,10] and core-level spectroscopy.[5,11,12] The first peak in the B $1s$ excitation spectra has been interpreted as a core exciton.[12] Its intensity is strongly dependent on the polarization of the incident light because the final state is π. However, it is not completely extinguished for $\vec{E} \perp \vec{c}$, indicating a small σ component in the final state. The origins of this σ-π mixing have not been explained and our understanding of the core spectra has been hampered to an extent by inconsistencies in the available band calculations.[12-16] We present a new three-dimensional tight-binding (TB) band structure which is consistent with various valence-band densities of states and employ it to describe the B and N core spectra. We study the binding energy and localization of the core excitons using a real-space defect Green's-function technique.[17,18] We find the σ-π mixing to be caused by the delocalized character of the exciton in $\vec{k}$ space and the contributions of states of smaller $k_{||}$ have larger σ-π mixing.

The electronic states of h-BN are enormously simplified by the high lattice symmetry. The mirror plane within each layer separates its single-layer bands into states of even (σ) and odd (π) parity.[13] The σ states are responsible for the strong covalent bonding within each layer. Also, the D_{3h} symmetry of each layer forces the cancellation of phase factors for all B-N interactions at the zone boundary, point P, producing a completely ionic minimum direct gap at this point, with N $p\pi$ valence states and B $p\pi$ conduction states. We expect the π states to dominate most excitation spectra as there are no σ states within 3 eV of either extrema. In three dimensions some σ-π mixing is allowed for finite $k_\perp$, but still no B-N mixing is allowed along the symmetry line KH.

The core exciton is further constrained because the immobile core hole requires the final electron state to have a definite point symmetry about the core excited atom. This final state must have p-like symmetry because of the $l \rightarrow l \pm 1$ atomic selection rule and either A_1^- (π-like) or E^+ (σ-like) point symmetry due to the lattice. We calculate the binding energy of the B $1s$ and N $1s$ core excitons for both Coulombic and central-cell core-hole potentials. We find the B $1s$ A_1^- exciton to be bound only when the full Coulombic potential is included. The final-state wave function is then calculated to find its localization and the source of the σ-π mixing.

The currently available band structures for h-BN give very diverging widths for some bands; for example, the computed widths of the crucial π bands differ by a factor of 4.[13-16] An experimental density of σ and π states has been extracted from the x-ray emission spectra.[8] Overall, the orthogonalized-plane-wave (OPW) results[14] resemble these spectra most closely but they still overestimate the π width, while the various TB results severely underestimate it. We calculate the bands for h-BN by transferring the TB interactions from graphite,[19] whose electronic structure is much better understood.[20] This resolves many of the questions for h-BN. We find that the π bands are anomalously wide because the π interaction between two p_z orbitals is almost twice that between two $p_{x,y}$ orbitals, indicating the σ and π orbitals to have very different spatial extents.

II. FITTING THE BAND STRUCTURE

Hexagonal BN has a lattice of D_{6h}^4 symmetry with $a = 2.504$ Å and $c = 6.66$ Å, and is illustrated in Fig. 1. Each boron atom is surrounded by three N atoms at 1.45 Å and also has six second-neighbor borons at 2.504 Å within one layer. The interlayer spacing of 3.33 Å is extremely large compared to the bond length within the layers. Consecutive layers are stacked directly over each other after inversion so that opposite species lie next to each other. There are also six important second-neighbor sites on adjacent layers at 3.63 Å of the same species. Graphite is isoelectronic to BN. It has a similar layer structure and a similar bond length, 1.425 Å, but the stacking arrangement of its layers differs slightly—the second layer is shifted one unit along the a axis, causing half of the sites to lie over holes on adjacent layers. Boron nitride also has a cubic zinc-blende polytype (zb-BN) with cell length $a = 3.165$ Å and bond length 1.565 Å.

The band structure of h-BN is to be calculated by fit-

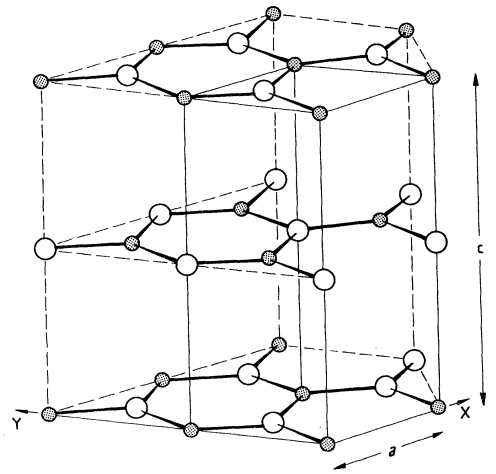

FIG. 1. Crystal structure of h-BN.

ting the TB parameters to experimental data or previous calculations. In the absence of reliable data for h-BN, the interactions are assigned by transferring from fitted band structures of similar compounds: graphite or zb-BN. The parameters derived from each source produce surprisingly different results and we give arguments to support those from graphite.

The TB parameters for graphite were derived by fitting[19] the linear combination of atomic orbitals (LCAO) bands of Painter and Ellis for a single layer of graphite.[20] An orthonormal s/p basis was used. The orbital energies are defined as $E(s)$ and $E(p)$, and all first-neighbor two-center interactions are included: $V(ss)$, $V(sp)$, $V(p\sigma)$, and $V(p\pi)$. The TB parameters are found by equating algebraic expressions for the band energies at Γ and K to the energies found by the LCAO calculation.[19,20] This ensures a very close similarity of our TB bands to the LCAO bands.[20] We find that the π interaction between the $p_{x,y}$ and p_z orbitals must be allowed different values, $V(p_x,\pi)$ and $V(p_z,\pi)$, respectively. Additionally, a few second-neighbor interactions are retained: A σ interaction between two p_x orbitals, $V_2(p\sigma)$, is needed to describe the upward dispersion of σ^* bands towards K, and a positive π interaction between two p_z orbitals, $V_2(p_z,\pi)$, which allows the π^* conduction band to be broader than the π valence band and represent the neglected overlap effects. The parameters for graphite are collected in Table I.

The two-center interactions of graphite were transferred directly without scaling to h-BN as their bond lengths are so close. We ignored possible differences in the second-neighbor B-B and N-N parameters. We also ignored the asymmetry of V(sc,pa) and V(sa,pc) as it was found to be minimal in zb-BN. New orbital energies are needed for BN. The difference of B and N p-orbital energies is set to the experimental optical gap, 4.3 eV,[1,21] as it is entirely ionic. The s energies are taken from atomic Hartree-Fock values and adjusted slightly to place the N 2s peak at the energy seen in x-ray emission.[8]

The TB parameters derived from fitting the bands of zb-BN (Ref. 22) differ considerably from those for h-BN (Table I). It is immediately apparent that the π interaction between p_z states is 1.6 times that between $p_{x,y}$ states in h-BN and over 2.7 times the π interaction in zb-BN. This illustrates the important structural dependence of TB interactions first found for cubic lattices.[23] Clearly, the p_z orbitals in layer structures have a much greater spatial extent than their $p_{x,y}$ orbitals and also of p orbitals in diamond lattices. The p_z orbitals point into the large interlayer region where they are presumably much less contracted by overlap repulsion than the σ orbitals. This structure dependence shows the importance of using "universal" TB parameters within similar bonding symmetries rather than within the same compound. This applies particularly to surface studies. The LCAO calculation for graphite[20] was able to reproduce this anisotropy because it used a double-ζ variational approach. Angle-resolved photoemission verified the calculated band dispersions.[24]

The interlayer dispersions are reproduced by retaining three interlayer interactions: a B-N interaction along the c axis and the B-B and N-N second-neighbor interactions. The D_{6h}^4 symmetry prevents the B-B and N-N interactions from producing any dispersion along the KH line where

TABLE I. Interactions (in eV) for graphite h-BN and zb-BN. No asymmetry is found for $V(sp)$ in zb-BN but an asymmetry is included between the interlayer B-B and N-N $V(p_z,\sigma)$ interactions. An sp^3s^* parametrization is used for zb-BN (Ref. 18), with $E(B,s^*)=E(N,s^*)=14$ eV and $V(s^*,p)=1.82$ eV.

		E(B,s)		E(B,p)	E(N,s)	E(N,p)	
Graphite		−3.75		0.48	−3.75	0.48	
h-BN		−0.5		4.78	−9.3	0.48	
zb-BN		1.3		7.5	−8.5	3.3	
Interaction	r,Å	$-V(ss)$	$V(sp)$	$V(p\sigma)$	$-V(p_x,\pi)$		$-V(p_z,\pi)$
h-BN intralayer	1.43	5.18	5.34	5.79	1.72		2.92
intralayer	2.50			0.28			−0.16
interlayer	3.33			0.13			
interlayer	3.63			−0.22 (B), −0.11 (N)			
zb-BN	1.53	3.68	4.81	5.82	1.05		

only the less effective B-N interactions are operative. All three types are effective away from symmetry line KH and the like-atom interactions dominate at Γ. The three interactions were chosen to reproduce the symmetry orderings of Doni *et al.*[13] and the bandwidths were fitted to reproduce the OPW results[14] at Γ. As the B-B and N-N $p\sigma$ interactions in Table I are negative, we feel that further calculations would be useful to confirm these values. Negative values are needed to broaden the π^* band more than the π band, but if the reverse turns out to be true, as in graphite,[20] then this corresponds to positive values.

III. BANDS OF *h*-BN

The bands and partial density of states (DOS) are shown in Figs. 2 and 3. All bands are doubly degenerate along the symmetry lines AH and AL. The π and π^* bands can be traced from the band extrema at point K to the $2^-,3^+$ states at point Γ. The p-like σ and σ^* bands form doubly degenerate 5^+ and 6^- states at point Γ which cannot be separated in Fig. 2. They form quadruply degenerate states at point A. The s-like states have 1^+, 4^- symmetry at Γ. Overall, there is reasonable agreement with the DOS extracted from x-ray and photoemission measurements.[8,4,5] The valence π band is found to be 5.95 eV wide, slightly narrower than deduced from x-ray emission (7.9 eV).[8] The lowest $p\sigma$ band extends down to -12.1 eV, similar to x-ray emission, but we find its maximum Γ_6^+ to be much lower, -2.9 eV compared to -0.4 eV. Our bands are closest to the OPW results,[14] particularly for the σ bands. In contrast, TB results[13,15,16] show much narrower π bands, frequently with a gap between σ and π states.

The gap is found to be direct at H but the KH dispersion is exceedingly small with our parameters. The π and π^* bands retain the asymmetry they possessed in graphite, with widths of 5.95 and 9.4 eV in h-BN. The dispersion along ΓA of the π^* band is 2.3 times larger than that of the π band. The states along KH are completely ionic, as mentioned in the Introduction. Elsewhere, their separation and covalent character increases with $V(p_z,\pi)$. We find the states along ΓA to be only 25% ionic because of our large $V(p_z,\pi)$ interaction, but previous TB calculations underestimated their bandwidths and overestimated their ionicity.

The σ^* states are quite flat in Fig. 2. Both the σ^* and s^* bands dip below the π^* bands at Γ. The s^* is higher than σ^* in h-BN, as in graphite and diamond. The flatness of the σ^* bands produces a strong peak in the DOS around 10 eV (Fig. 3). We believe the lower σ^* band will remain flat in calculations using a larger basis and the peak will remain, while the upper σ^* band may curve upwards, as in the OPW results.

IV. CORE EXCITONS

Excitations of core electrons differ from those of valence electrons in that the core hole is assumed to be infinitely massive, remaining trapped on its original atom for the lifetime of the exciton. This hole localization causes core spectra to retain many atomiclike features, particularly the $l\rightarrow l\pm1$ selection rule.[25] The atomiclike character of the transitions can be seen from the optical constant ϵ_2,

$$\epsilon_2(\omega)\propto\omega^{-1}\sum|\langle i|x|f\rangle|^2 . \tag{1}$$

The matrix element between initial and final states

$$M=\langle i|x|f\rangle \tag{2}$$

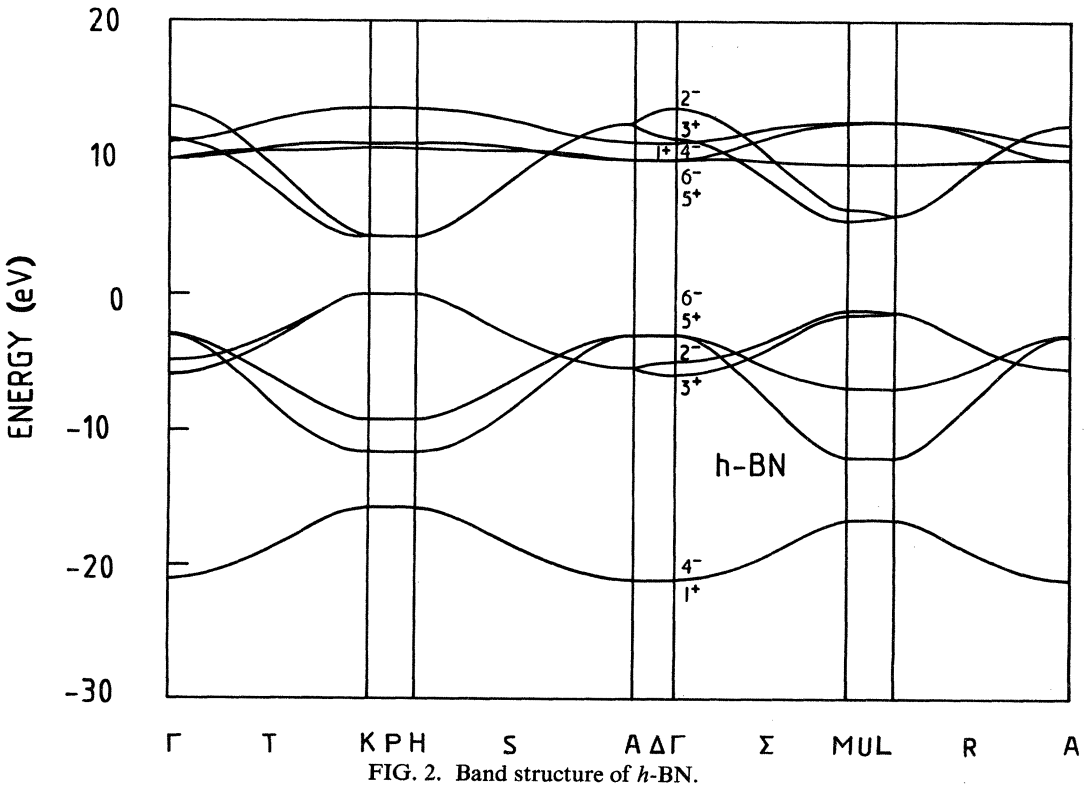

FIG. 2. Band structure of h-BN.

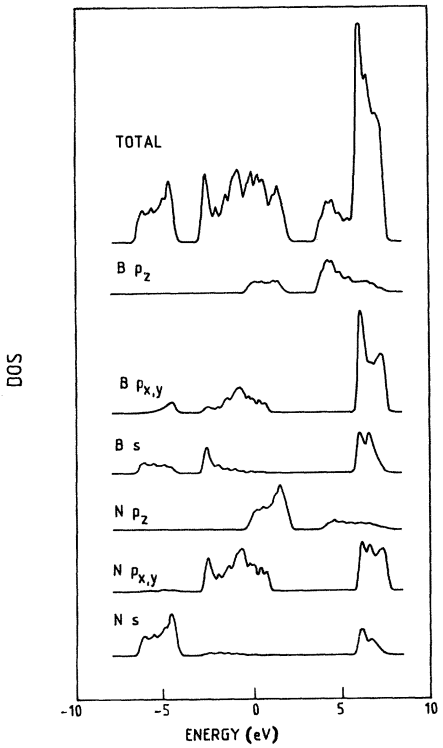

FIG. 3. Total and partial DOS for h-BN.

is extremely localized because the product $x\,|\,i\rangle$ only extends as far as the core state itself. Thus the 1s cores couple to $|\,f\rangle$ in proportion to its p-like component of that site at energy ω.

The core-hole potential usually binds exciton states below the threshold for core-to-band transitions. These core excitons often have much larger binding energies than the corresponding valence excitons. While the core hole is always localized, the excited electron can be localized or spread out, as in the Frenkel and Wannier extremes. This transition is similar to that from deep to shallow for impurity states in semiconductors.[17,18] Deep impurity levels have recently been defined as states bound only by the central-cell part of the total impurity potential. Shallow centers are those bound by the long-range Coulombic tail. In a similar manner core excitons are defined as deep if the central-cell potential binds the state. Otherwise, a conduction-band resonance, referred to as a "deep resonance," is found. Deep resonances are also strongly localized in their central cells.

The oscillator strength of excitonic features is proportional to the central-cell amplitude of their final state via M [Eq. (2)]. The core hole always localizes a deep state, whether in the gap or resonant. It also always produces shallow-gap states even if they are only the excited state of a deep-gap state. In well-screened semiconductors, the shallow states have small central-cell weight and lie close to the band edge. The deep resonances are often visible in core spectra as excitonically enhanced conduction-band features but the shallow states are not observed. Thus in semiconductors a clear transition from bound to resonant core excitons is seen experimentally at the cation site in the series GaP-GaAs-GaSb (Refs. 17 and 26) and in GaS-GaSe-InSe.[27,28] The central-cell potential largely determines the binding energy of the core exciton in semiconductors and the rest of the Coulombic tail has only a minor effect of order 0.1 eV because of the large ϵ. In contrast, insulators have small ϵ and even nominally "shallow" states have large binding energies and compact wave functions with relatively large central-cell amplitudes. Their gap states are readily observed in core spectra. Also in insulators, while the central-cell potential has a large effect on the binding energy, the Coulombic tail can no longer be neglected due to the poor screening.

There are a number of possible core excitons in h-BN, each with different point symmetries and σ-π contents. The final states have A_1^- or E^+ symmetry about B or N for transitions from B or N 1s levels. Their oscillator strengths are proportional to the p content and their polarization behavior depends on their σ and π content.

We find the core excitons of h-BN to be small as in other insulators. The Bohr radius and binding energy can be estimated in the effective-mass model to be 1.1 Å and 1.5 eV, respectively, assuming $\bar{\epsilon}_\infty = 4.5$ (Ref. 29) and $\bar{m}^* = 2.2 m_0$.[12] This radius is quite small compared to the bond length of 1.43 Å so clearly the effective-mass limit is inapplicable. Screening in h-BN is surprisingly isotropic with $\epsilon_{||} = 4.1$ and $\epsilon_\perp = 4.95$ experimentally,[29] but the binding energy is much larger than the π^* dispersion along KH, so the exciton cannot be treated as three dimensional, as in Ref. 12.

Altarelli *et al.*[30] studied excitons of general binding energy. They expressed the two-particle wave function of the exciton in terms of the Green's function of decoupled valence and conduction bands. Here, the localization of the core hole allows its potential to be approximated by the potential of the positive ion of the next heavier element in the Periodic Table, the $Z+1$ approximation.[31] This approximation transforms the two-particle exciton equations to those of a single particle, the excited electron. It also defines the potential in a very valuable manner, although it simplifies any core-relaxation effects.

We employ a real-space Green's-function technique to calculate the binding energy and wave function of the core excitons. The binding energy E is found as the solution of a secular equation involving the multiband Green's function,

$$\det |\, \mathbb{1} - \underline{G}(E)\underline{V} \,| = 0 \,. \tag{3}$$

The Green's-function operator G is constructed in the gap as a sum over all bands at 20 special points,

$$G(E) = \sum_{i,\mu} |\, E - E(\vec{k}_i)]^{-1} \,|\, \mu, \vec{k}_i \rangle \langle \mu, \vec{k}_i \,| \;,$$

where $E_\mu(\vec{k})$ are the band energies and $|\,\mu, \vec{k}_i\rangle$ is a Bloch state of wave vector $\vec{k}$ for the μth band.

We consider initially the semiconductor limit and the central-cell binding of the B and N 1s excitons. In this limit we retain only the on-site part of the defect potential V. V is diagonal because the off-diagonal terms vanish, as they are assumed to depend only on bond lengths which are unchanged in core excitation. Each diagonal term is

the difference of the orbital energies of the $Z+1$ impurity and the host. For the 1s B exciton the C and B difference is set to half the ionic optical gap, -2.15 eV, to exclude further adjustable parameters. For the N core exciton, the N-O difference is -2.65 eV. The solutions of (3) can be factored by the symmetry of the B and N sites. The s, $p_{x,y}$, and p_z orbitals belong to A_1^+, E^+, and A_1^- representations.

The core-exciton binding energies are found by solving the scalar equations

$$V_l = 1/G_l(E)$$

in the central-cell limit, and are plotted against V_l in Fig. 4. The B A_1^- exciton is seen to be the most strongly bound of the various excitons, but even this is borderline resonant at $V=-2.15$ eV. The N A_1^- curve (not shown) has no negative solution in the gap and has no solutions in the lower conduction bands for $V_l=-2.65$ eV, corresponding to the O impurity. The E^+ levels possess resonant solutions high in the conduction band. These lie below the σ^* bands from which their states derive. We explain below that the resonant character of the B A_1^- exciton is due to the overall covalence of the π^* states, and then show that it is bound by the longer-range part of the core-hole potential.

The qualitative behavior of the central-cell solutions of Fig. 4 can be understood in terms of the impurity molecule model of the core site and its immediate neighbors.[17] Each solution for this model is a hyperbola with a horizontal asymptote and a diagonal asymptote of unity slope. The electron lies on the upper branch. Its character depends on the host ionicity only via the movement of the horizontal asymptote. In the covalent limit the asymptote or pinning level lies near midgap. In the ionic limit its energy is roughly that of the orbitals on the adjacent site, N for the case of B. This model predicts that core excitons at B should be much deeper than those at N. Thus a deep bound B 1s exciton might be expected, in view of the ionic minimum of h-BN. Figure 4 shows that the deep exciton is not "bound."[32] This occurs because a deep exciton mixes states away from KH which are significantly less polar. The impurity model demonstrates the importance of π^* bandwidth and accounts for our earlier emphasis on obtaining the correct intralayer and interlayer dispersions.

Although the B exciton is not deep, it is still compact and our real-space Green's-function method is easily extended to study its localization and polarization. We extend the basis of A_1^- states about the B site by including symmetrized orbitals for 17 shells of neighbors (out to 6.7 Å) or perhaps 6 times the effective-mass radius), nine shells in the same layer, five in the adjacent layer, and three in the next. The potential V is taken to be screened Coulombic with $\epsilon=4.5$ outside the first shell. There are now a number of solutions of (3) for the A_1^- states which represent the ground state and the excited shallow states. The ground-state energy for 17-shell binding and central-cell binding are compared for increasing central-cell potential in Fig. 5 for the B A_1^- exciton. In the central-cell case the exciton changes from resonant to bound for $V<-2.6$ eV. In the extended potential case, the ground state is always bound and changes from shallow to deep for V less than about -2 eV. We find a binding energy of 0.5 eV for the B A_1^- exciton when 17 shells are retained. This compares with experimental values of 1.9 eV from a line-shape analysis and 0.8 eV from placing the B 1s line by photoemission and taking the optical gap as 4.3 eV.[12]

The delocalized nature of the exciton is the cause of the σ-π mixing in the final A_1^- state. The type of mixing allowed is severely constrained by the lattice symmetry. The A_1^- level cannot contain any σ states from the same layer as the core hole. Thus it is insufficient to consider interband mixing in the single-layer bands. We find the main σ-π mixing to arise from the second-neighbor borons on adjacent layers through the B-B interlayer interaction. However, the phase factors are easily shown to cancel along KH, so this source of mixing is prevented at the conduction-band minimum itself, but is allowed towards

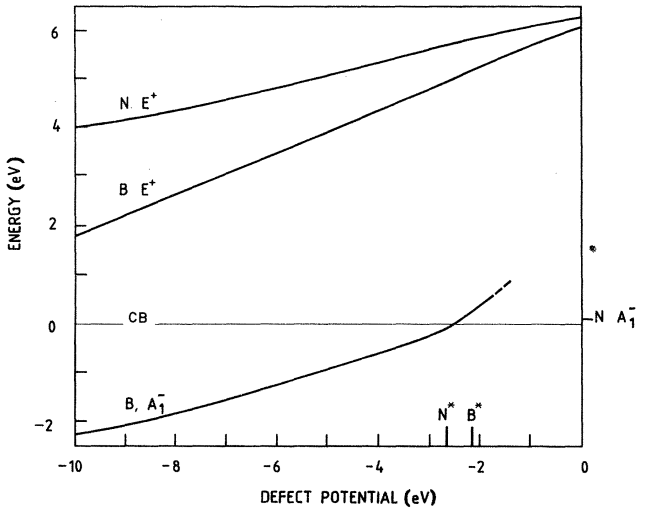

FIG. 4. Calculated B 1s and N 1s core-exciton binding energies as a function of the central-cell hole potential.

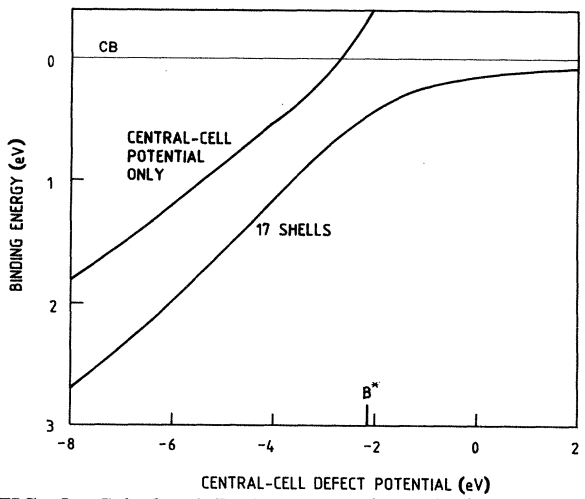

FIG. 5. Calculated B A_1^- core-exciton binding energy for varying central-cell potential: (a) central-cell potential only, and (b) screened Coulombic potential out to 17 shells.

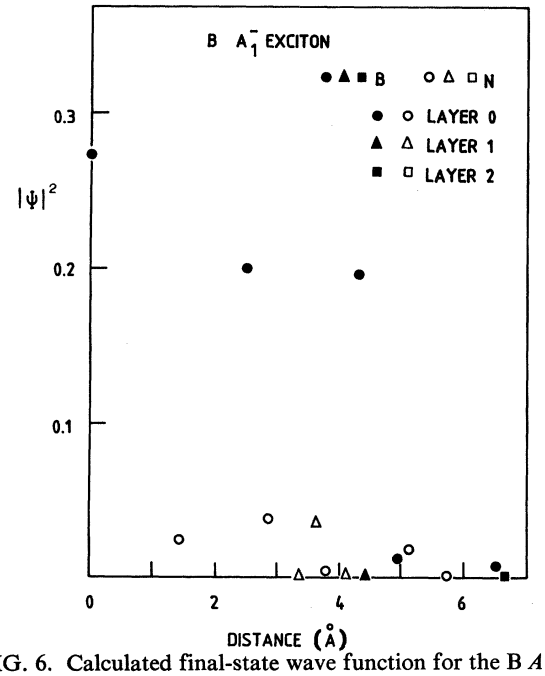

FIG. 6. Calculated final-state wave function for the B A_1^- exciton.

ΓA. Thus, σ-π mixing is largely due to the exciton delocalization in $\vec{k}$ space away from the KH direction.

The final-state wave function can be studied quantitatively by the Green's-function technique[33] by noting that the proportion of a localized state $|j\rangle$ in the final state $|f\rangle$ is found from

$$\frac{\delta E}{\delta V_j} = |\langle j|f\rangle|^2 .$$

Figure 6 shows the B A_1^- exciton to have its greatest intensity in the central cell (0.27) and on the nearest in-plane B neighbors (0.20). Considering the rate of decay on B sites within the layer, the exciton is found to have a radius of 3 Å. The amplitude has become negligible by the second layer. The results also confirm our qualitative discussion of σ-π mixing. A 0.3% contribution of σ states on the second-neighbor interlayer boron site is found and we estimate an overall 0.5% σ content. However, this is less than derived experimentally from the exciton's polarization dependence.

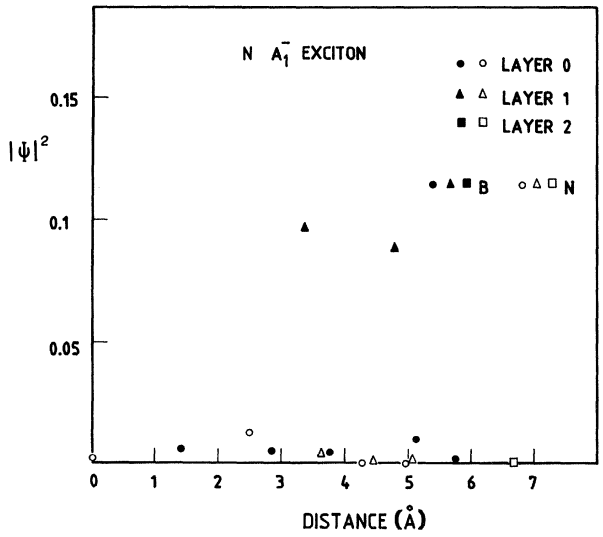

FIG. 7. Calculated final-state wave function for the N A_1^- exciton.

The N 1s exciton can be studied in a similar fashion. No deep exciton is found in the central-cell limit. A shallow A_1^- exciton binding energy of about 0.1 eV is found for 17 shells of Coulombic binding. The electron wave function has also been calculated (see Fig. 7). In this case, there is little weight on the central cell (0.04) and the greatest amplitude is found on the adjacent-plane B neighbors. Experimentally, the N 1s exciton has a negative binding energy, estimated from a core-level position of 402 eV and a gap of 4.3 eV.[6,9] Experimentally, it is also polarization dependent,[9] as expected from the π-like final state.

The binding energies for both B and N shallow excitons in h-BN are much smaller than the effective-mass estimate. This is largely due to the lattice symmetry preventing many shells from contributing to their binding.

We may interpret the core spectra above the edges in terms of the conduction-band partial DOS and the resonant exciton levels. The principal transitions from the B 1s or N 1s cores for light-polarized $\vec{E}\perp\vec{c}$ are to the flat σ^* conduction bands 6 eV above the edge. The B $1s\rightarrow p_z$ transition for $\vec{E}\|\vec{c}$ is to the broader π^* conduction band. We assign the strong twin-peaked structure at 199–200 eV in the B 1s core absorption spectra for $\vec{E}\perp\vec{c}$ (Refs. 5 and 12) to transitions to the two σ^* bands, and the shallower peak at 204.5 eV to transitions to the upper σ^* band away from point Γ. We predict a strong polarization dependence of the 200-eV peak, with a broader somewhat lower-energy peak expected for $\vec{E}\|\vec{c}$, as is seen.[12] The N 1s spectra should show similar features to the B 1s spectra because the N p admixture in the σ^* and π^* is not strongly energy dependent away from point K. Broadly speaking, this is observed in the lower-resolution data.[6]

V. DISCUSSION AND CONCLUSIONS

Experimentally, core excitons are more strongly bound at cation sites than anion sites in ionic solids.[34] However, their conduction bands are poorly described by TB Hamiltonians. The lattice symmetry of h-BN produces an ionic minimum gap and provides what appears to be a unique opportunity to study core excitons within an ionic gap in an essentially covalent material, whose band structure is well described by TB methods. For covalent materials, a combination of an accurate band structure, the $Z+1$ approximation, and the defect Green's-function method provide an accurate means to study their core excitons. The stronger binding of cation core excitons is easily derived from the impurity molecule model. A deep A_1^- core exciton could be expected at the boron (cation) site in h-BN. However, states over a wide energy range participate in deep levels, so the overall covalent character of the π^*

band causes this exciton to be borderline resonant in the central-cell limit.

The layer symmetry of h-BN also allows a sensitive measurement of the final-state wave function.[12] Its qualitative features were calculated using the Green's function. Quantitatively, $|f\rangle$ and the binding energy depend quite strongly on the accuracy of the band structure. We are confident the intralayer interactions are correctly represented here, but there remain some doubts over our values for interlayer interactions. Perhaps the largest uncertainty in the core exciton is its experimental binding energy, which arises, surprisingly, because there is no widely accepted value for the optical gap.

The influences on the band structure of single layers of h-BN and graphite are now better understood. We pointed out that the π overlap of the p_z orbitals is much greater than that of the $p_{x,y}$ orbitals which leads to quite large π bandwidths.

Zunger has recently developed a self-consistent pseudopotential Green's-function theory of deep-core excitons[35] which is complementary to the present TB approach, in the same manner that theories of real defects have developed.[18,36] Zunger also noted the importance of a valence polarization effect which acts to increase the apparent core-exciton binding energy when this is determined experimentally by positioning the core level by photoemission; this effect has been omitted or only noted in previous theories. Work is in progress to include this term in our TB approach, but in view of the large experimental uncertainty of the binding energies for h-BN, this does not affect our principal conclusions.

ACKNOWLEDGMENTS

The author is pleased to acknowledge many fruitful conversations with Professor F. C. Brown and Professor J. D. Dow, and the support of the U. S. Navy Office of Naval Research (Contract No. N00014-79-C-0537).

*Present address: Central Electricity Research Laboratories, Leatherhead, Surrey KT22 7SE, United Kingdom.

[1]J. Zupan and D. Kolar, J. Phys. C 5, 3097 (1972).
[2]A. Zunger, A. Katzir, and A. Halperin, Phys. Rev. B 13, 5560 (1976).
[3]R. Mamy, J. Thomas, G. Jezequel, and J. C. Lemonnier, J. Phys. (Paris) Lett. 42, L-473 (1981).
[4]D. J. Joyner and D. M. Hercules, J. Chem. Phys. 72, 1095 (1980).
[5]J. Barth, C. Kunz, and T. M. Zimkina, Solid State Commun. 36, 453 (1980).
[6]V. A. Fomichev and M. A. Rumsh, J. Phys. Chem. Solids 29, 1015 (1968).
[7]E. Tegeler, N. Kosuch, G. Weich, and A. Faessler, Phys. Status Solidi B 84, 561 (1977).
[8]E. Tegeler, N. Kosuch, G. Weich, and A. Faessler, Phys. Status Solidi B 91, 223 (1979).
[9]R. D. Leapman and J. Silcox, Phys. Rev. Lett. 42, 1361 (1979); R. D. Leapman, P. L. Fejes, and J. Silcox, Phys. Rev. B 28, 2361 (1983).
[10]U. Buchner, Phys. Status Solidi B 81, 227 (1977).
[11]F. C. Brown, R. Z. Bacharach, and M. Skibowski, Phys. Rev. B 13, 2633 (1976).
[12]B. M. Davies, F. Bassani, F. C. Brown, and C. G. Olson, Phys. Rev. B 24, 3537 (1981).
[13]E. Doni and G. Pastori Parravicini, Nuovo Cimento 64B, 117 (1969).
[14]M. S. Nakhmanson and V. P. Smirnov, Fiz. Tverd. Tela (Leningrad) 13, 2383 (1971) [Sov. Phys.—Solid State 13, 2763 (1971)].
[15]J. Zupan, Phys. Rev. B 6, 2477 (1972).
[16]R. Dovesi, C. Pisani, and C. Roetti, Int. J. Quantum Chem. 17, 517 (1980).
[17]H. J. Hjalmarson, H. Buttner, and J. D. Dow, Phys. Rev. B 24, 6010 (1981); J Robertson, Phys. Rev. B 28, 3378 (1983).
[18]H. J. Hjalmarson, P. Vogl, Wolford, and J. D. Dow, Phys. Rev. Lett. 44, 810 (1980).
[19]J. Robertson, Philos. Mag. B 47, L33 (1983).
[20]G. S. Painter and D. E. Ellis, Phys. Rev. B 1, 4747 (1980); R. F. Willis, B. Fitton, and G. S. Painter, Phys. Rev. B 9, 1926 (1974).
[21]There are some widely diverging experimental values for the minimum optical gap of h-BN. A value of 4.3 eV is taken from the steep onset of transitions quoted in Ref. 1 which is only seen as a tail in Ref. 2. This value is also quoted in x-ray emission work (Ref. 6).
[22]A. Zunger and A. J. Freeman, Phys. Rev. B 17, 2030 (1978).
[23]S. Froyen and W. A. Harrison, Phys. Rev. B 20, 2420 (1979).
[24]P. M. Williams, Nuovo Cimento 38B, 216 (1977).
[25]T. Alberg and J. L. Dehmer, J. Phys. C 6, 1450 (1973).
[26]D. Aspnes, M. Cardona, V. Saile, M. Skibowski, and G. Sprussel, Solid State Commun. 31, 99 (1979).
[27]M. Piacentini, C. G. Olson, A. Balzaroffi, R. Girlanda, V. Grasso, and E. Doni, Nuovo Cimento 54B, 248 (1979).
[28]J. Robertson, J. D. Dow, and M. Piacentini (unpublished).
[29]R. Gieck, C. H. Perry, and G. Rupprecht, Phys. Rev. 146, 543 (1966).
[30]W. Andreoni, M. Altarelli, and F. Bassani, Phys. Rev. B 11, 2352 (1975).
[31]J. D. Dow, D. R. Franceschetti, P. G. Gibbons, and S. E. Schnatterly, J. Phys. F 5, L211 (1975).
[32]The lack of central-cell binding of the B 1s exciton is unlikely to be caused by the inapplicability of the defect GF method to h-BN. h-BN is a strongly covalent material. Its electronic states around the gap are very well described by our limited-basis TB theory. There is much less free-electron character or excited-state contributions to its lower conduction bands in h-BN than in more isotropic semiconductors such as Si. This can be judged from the band structure of graphite at higher energies (Ref. 20) where the higher bands are reasonably separated from those derived from $2s,2p$ states.
[33]The localization of deep impurity states have been studied in a similar manner by S. Y. Ren, O. F. Sankey, and J. D. Dow, Phys. Rev. B 26, 951 (1982).
[34]S. T. Pantelides, Phys. Rev. B 11, 2391 (1975).
[35]A. Zunger, Phys. Rev. Lett. 50, 1215 (1983).
[36]For example, U. Zindefelt and A. Zunger, Phys. Rev. B 26, 896 (1982); M. Scheffler, in *Festkorperprobleme*, edited by P. Grosse (Vieweg, Braunschweig, 1982), Vol. 22, p. 115.